Int. J. Heat Mass Transfer. Vol. 32, No. 6, pp. 1175–1182, 1989
Printed in Great Britain

0017–9310/89 $3.00+0.00

The effect of geometry on the performance of the closed tube thermosyphon at low Rayleigh numbers

G. S. H. LOCK and Y. LIU
Department of Mechanical Engineering, University of Alberta, Edmonton, Alberta, Canada T6G 2G8

(*Received* 10 *May* 1988 *and in final form* 29 *November* 1988)

Abstract—The results of an experimental investigation of heat transfer in the closed tube thermosyphon under laminar conditions are presented. Attention is focused on the effect of tube geometry when the Rayleigh number is low enough to create boundary layer, transitional and impeded flows. The data show that the length–diameter ratio and heated–cooled length ratio both have a monotonic effect on the heat transfer rate, the former being the greater. Results are presented for both air and water, with the latter tests including the effect of cooled wall temperatures low enough to produce an inverted flow in the cooled section.

INTRODUCTION

SINCE its advent as a device capable of cooling gas turbine blades, the tubular thermosyphon has been the subject of much study. It takes on two separate though related forms. The open thermosyphon consists of a heated tube sealed at the bottom but open at the top where a discharging annulus of warm fluid surrounds an entering core of cooler fluid. The closed thermosyphon is simply two open thermosyphons joined at their open ends, the lower tube being heated and the upper one being cooled. This paper is concerned only with the latter form under single-phase conditions.

In recent years, the device has been applied to the freezing of moist soil and water streams in northern climates [1, 2]. Cold winter air extracts heat through the natural circulation set up in the system, and thereby removes latent (and sensible) heat from the material surrounding the buried or submerged part of the tube. In this application, the tube is filled with a fluid that does not freeze but circulates in a manner determined by the tube geometry and, for single-phase conditions, by the Rayleigh number.

The behaviour of the closed system was first studied by Bayley and Lock [3] who demonstrated that there were two principal flow regimes. At high Rayleigh numbers, a thin, annular boundary layer forms adjacent to the tube wall, moving away from the closed end; a larger, relatively slow moving core travels in the opposite direction. This boundary layer regime persists down to $t_d \simeq 10^5$, where $t_d = Ra_d\, d/L_H$. Below this value, further reductions lead to increasing interference between the core and the annular layer in an impeded regime. Also noted in ref. [3] was the appearance of a dramatic chasm in the impeded regime when the tube was filled with air.

Chasmic behaviour had been observed earlier in an air-filled open thermosyphon [4]. Subsequent work on the open air system has not been extensive [5–7] despite the obvious availability of air as a fluid which does not readily freeze. Work on the closed system appears to have focused almost exclusively on liquid fillings under conditions where the Rayleigh number was large enough to create turbulent flow, although some data do extend down into the laminar boundary layer regime [3, 8–10].

Apart from the intrinsic merit of studying the unknown low Rayleigh number behaviour of the closed tube thermosyphon, the performance of the device in this range represents a conservative estimate suitable for design purposes. In view of the lower heat transfer rates normally associated with the impeded regime, and the additional prospect of chasmic behaviour, it would seem worthwhile to investigate the severity and extent of the heat transfer deterioration. Accordingly, the present study, using small diameter tubes, was undertaken with the general objective of exploring regime behaviour and the particular aim of uncovering the effect of a wide range of tube geometries on heat transfer efficiency.

EXPERIMENTAL CONSIDERATIONS

The rig

The experiments were performed in a low temperature wind tunnel in which the temperature could be adjusted in the range −20 to 10°C, and the air speed could be set at any value between 10 and 60 m s^{-1}. Copper thermosyphon tubes (1.96 cm i.d.) were inserted through the bottom panel of the octagonal test section, as indicated in Fig. 1, from which it is evident that the cold air in the tunnel provides the

NOMENCLATURE

d	tube diameter
g	gravitational acceleration
h	heat transfer coefficient
k	thermal conductivity
L	tube length
m, n	exponents
Nu_d	Nusselt number, hd/k
Pr	Prandtl number, ν/κ
Ra_d	Rayleigh number, $\beta g(T_H - T_C)d^3/\nu\kappa$
t_d	$Ra_d\, d/L$
T	absolute temperature.

Greek symbols

β	thermal expansion coefficient
Δ	depth of coupling region
κ	thermal diffusivity
ν	momentum diffusivity.

Subscripts

C	cold section
d	diameter
H	hot section
L	length
Δ	coupling region depth.

Superscript

*	transitional.

means by which heat is removed from the upper section of the thermosyphon.

The lower section of the thermosyphon tube was heated electrically using resistive tape wrapped over a layer of fibreglass tape previously wrapped around the outside of the tube (to provide electrical insulation). The heater windings were divided every 10 cm of tube length, each separate length being provided independently with power from the building mains and being controlled by means of a Variac transformer. The power delivered to the heater was measured in the usual way with a voltmeter and an ammeter.

The heated length of the thermosyphon was varied simply by attaching or detaching additional lengths using a threaded coupling piece. In the tunnel wall, the uppermost piece of the heated section fitted into a plexiglass hinge which served to connect the heated section to the cooled section without the copper tubes actually touching each other; this was helpful in simulating a temperature discontinuity between the two sections. Variations in the cooled length were effected with a plastic plug ($k = 0.25$ W m^{-1} K^{-1}) which prevented fluid access to the top region of the upper section, as shown in Fig. 1.

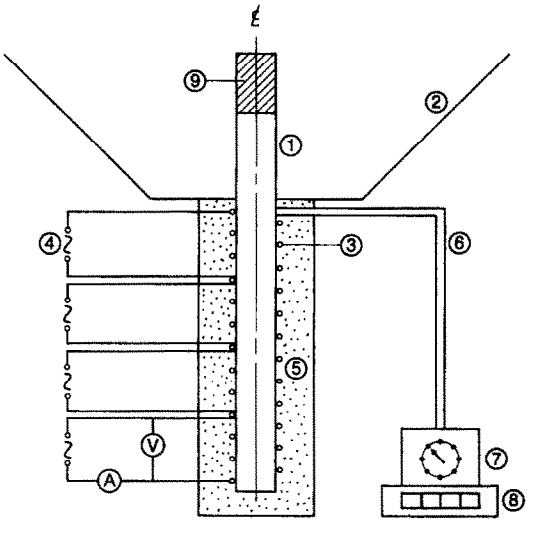

①Thermosyphon tube
②Wind tunnel wall
③Heater tape
④Power supply/control
⑤Thermal insulation
⑥Thermocouple leads
⑦Switching box
⑧Digital thermometer
⑨Plastic plug

FIG. 1. Schematic of apparatus.

Instrumentation and calibration

Temperature was measured throughout by means of thermocouples located in the airstream, the ambient air, and along the thermosyphon heated and cooled section walls at intervals of 5 cm. The tube thermocouples were installed on the outside of the wall prior to it being wrapped with the fibreglass tape mentioned earlier. The wires were led out along isotherms wherever possible and were connected to a Fluke 2175 A digital thermometer via a switching box.

During the tests, adjustments in the power being supplied to individual heaters made it possible to control axial variations in tube wall temperature. Prior to the tests the heated sections were calibrated in order to determine the heat leakage which had to be subtracted from the gross electrical power being supplied. This was done with the cooled section absent and the heated section filled with granular insulating material. Under such conditions, the gross power supply provides a good estimate of the heat leakage which was then plotted against the temperature difference between the heated tube wall and the ambient air. Most of the leakage is from radial conduction, but an attempt was also made to estimate the end leakage into the tunnel air by comparing results for various wind speeds and temperatures. As anticipated, this correction was small.

Wind speed was measured with a pitot-static tube but was not treated as an experimental variable. In

fact, the wind speed was fixed at 38 m s^{-1} in order to generate heat transfer coefficients around the cooled section which were high enough to promote a fairly uniform tube wall temperature both circumferentially and axially. No attempt was made to estimate the heat lost from the upper tube by convection because under the steady conditions studied it was assumed to be equal to the net heat supplied to the lower tube.

Procedure and test schedule

After the calibration runs mentioned above, the experiments were conducted as follows. The tunnel was switched on, and the air speed and temperature were set at predetermined values. While the tunnel was reaching thermal equilibrium (a period of 1–2 h) the tube heaters were switched on and the power set at some level in the anticipated range of the run. Tube wall temperatures at various locations on both the heated and cooled sections were then monitored and adjusted periodically in order to obtain an acceptable degree of uniformity. This was continued for a period of at least 3 h by the end of which the system had reached a steady state. Readings were then taken of the final tube temperatures, gross power supply, wind temperature and ambient temperature.

If these readings were considered satisfactory, the power level was adjusted and the procedure repeated, without changing the tunnel conditions. At the end of a run, the entire system was shut down and the thermosyphon tubes either exchanged or modified for the next run. Modifications included changes in heated length, cooled length, or filling fluid; water was used for most of the tests and air was used to explore regime behaviour.

Table 1 gives the complete range of the experimental variables. As indicated, the geometry was varied with $10 < L_H/d < 60$ and $1 < L_H/L_C < 12$, ranges which cover the majority of current applications. The experiments were limited to a fixed diameter tube and a range of Rayeligh numbers from 10^4 to 6×10^7.

DISCUSSION OF RESULTS

Flow behaviour

As noted elsewhere [3, 8, 11, 12], the closed tube thermosyphon may be viewed as a pair of open thermosyphons connected back to back. This is useful in the discussion of regime behaviour which is similar in the two systems. Both exhibit boundary layer regimes and impeded regimes, though not necessarily at the same time, and both reveal the chasmic transition discussed later. However, direct correspondence does not normally exist because of the mechanisms by which the open elements are coupled in the vicinity of the junction plane.

Figure 2 is a schematic representation of conditions in the coupling region. For small values of the temperature difference $T_H - T_C$, the isotherms within the fluid are as sketched in Fig. 2(a). Deep within either tube, the radial temperature gradient is steep near the wall and shallow in the interior which is occupied by the returning core. The axial temperature gradient steepens as the junction plane is approached: there it is a maximum, the magnitude increasing with radius. At the wall, the axial temperature gradient reaches its greatest value, and it is therefore near the wall that the presence of a Rayleigh (thermal) instability would be felt first and strongest.

In the absence of a thermal instability the fluid would tend to follow the pattern indicated in Fig. 2(b) which shows a purely refluent system; heat transfer between the two tubes is then solely by conduction across the junction plane. It is hypothesized that such a coupling mechanism would continue until a critical (transitional) value of $Ra_\Delta^* = \beta g(T_H - T_C)\Delta^3/\nu\kappa$, where Δ is the axial extent (depth) of the coupling region, has been attained. For $Ra_\Delta > Ra_\Delta^*$, the lower (hot) annulus of rising fluid must somehow cross through the upper (cold) descending fluid, and vice versa. This 'advective breakthrough' is shown schematically in Fig. 2(c). Such behaviour has been verified and discussed elsewhere [3, 8].

The situation is more complex with a pure water filling because of the inversion point near 4°C. Figure 3 illustrates the situation where the temperature difference across the thermosyphon is maintained at 4 K but the mean temperature is changed from 6 to 4

Table 1. Test schedule

Run	L_H (cm)	L_C (cm)	L_H/d	L_H/L_C	Fluid
1	20	20	10	1	Air
2	20	20	10	1	
3	40	20	20	2	
4	40	10	20	4	
5	80	20	40	4	Water
6	80	10	40	8	
7	120	20	60	6	
8	120	10	60	12	

$d = 1.96$ cm, $10^3 < t_d < 10^6$, $10^4 < Ra_d < 6 \times 10^7$.

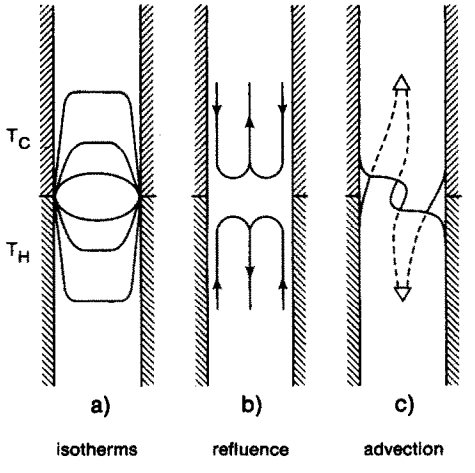

FIG. 2. Coupling behaviour.

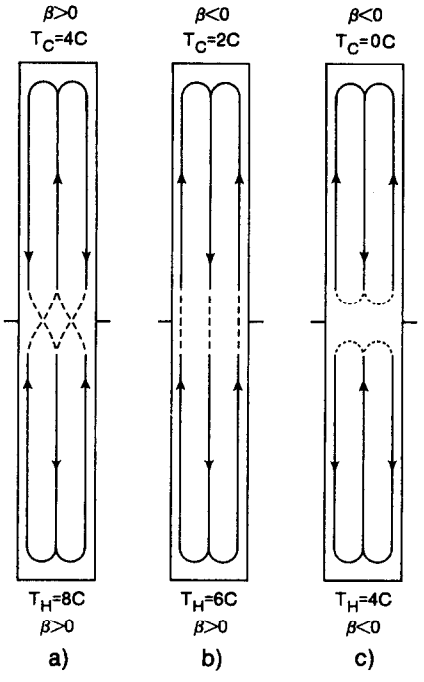

FIG. 3. Inversion effect with pure water.

to 2°C. In Fig. 3(a), the thermal expansion coefficient β is positive in both heated and cooled sections and the flow takes the 'conventional' form discussed above. Figure 3(b) shows that when β is positive in the heated section but negative in the cooled section, the annular and core flows do not change direction across the central plane at mid height. In Fig. 3(c), $\beta < 0$ throughout the entire system and hence the flow system in the heated section is once more the mirror image of that in the cooled section, both having undergone a complete flow reversal. It is thus clear that when β is positive in the heated section the coupling is wholly or partly advective whereas when β is negative in the heated section the coupling is conductive regardless† of the Rayleigh number.

The precise point of 'advective breakthrough' is not known, but it is reasonable to expect it to occur at a value of Ra_Δ much greater than the value associated with convective turnover between horizontal plates of different temperatures, i.e. $O(2\times10^3)$. Near $Ra_\Delta = Ra_\Delta^*$, the heat transfer rate would change rapidly with Ra_Δ (or t_d) but for $Ra_\Delta \gg Ra_\Delta^*$ the slope of the $\log Nu$–$\log t$ curve would tend to decrease with Ra_Δ, at least up to the point of transition‡ to turbulence.

Equally important is the fact that the advective mechanism will be associated with a secondary mixing process, the vigour of which will depend upon Ra_Δ, the Prandtl number and the size of the region within which the advective process occurs. Advection *per se* constitutes an improved thermal exchange mechanism over conduction, but secondary mixing can be expected to have a deleterious effect.

Figure 4 shows some of the air and water data of Table 1 plotted together with some air and water data from Bayley and Lock [3]. It is immediately apparent from this figure that the current air and water data are quite separate from each other by an amount which cannot be explained in terms of a simple Prandtl number dependency. It is also evident that the current data are consistently below those of ref. [3] even though the experimental conditions were similar. This latter fact is not easily explained, but may have been caused by a number of minor differences acting separately or collectively in conditions where Ra_Δ is quite low. For example, in the boundary layer regime at $t_d = O(10^6)$, $Ra_\Delta \simeq t_d^{1/4} L_H/d = O(10^{5/2})$, suggesting that refluence may have been significant, but both L_H/d and Ra_d were similar for the current data and those of ref. [3]. Alternatively, the explanation may lie in the boundary conditions: specifically in the axial temperature profile. In the present experiments, the tubes were made of copper and the two sections were separated from each other only by a small washer of insulating material ($k = 0.16$ W m^{-1} K^{-1}). These factors are likely to have produced smaller axial temperature gradients, particularly in the vicinity of the junction plane, than in ref. [3], and may therefore have created conditions less favourable for advective exchange.

It is interesting to note that increasing t_d would increase the effective Nusselt number of each section but would also increase fluid velocities and the degree of secondary mixing in the coupling region. Figure 4 reveals that for $t_d > O(10^5)$, these two opposing effects cancel each other and thereby render the overall Nusselt number essentially independent of t_d, at least up to 10^6.

Figure 4 also shows the chasmic air data of Bayley

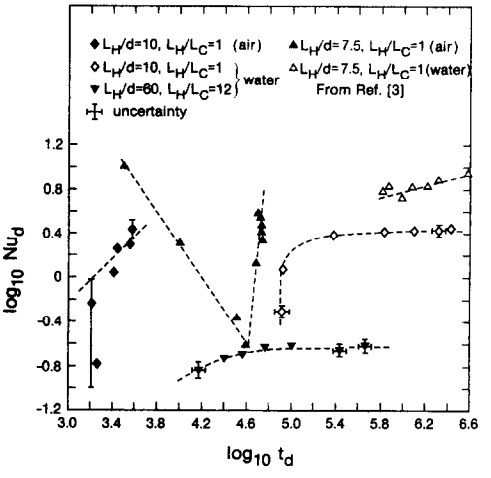

FIG. 4. Laminar regimes of closed tube thermosyphon.

† Assuming that the flow is not turbulent, when mixing would be important.

‡ Perhaps even beyond this point if it precipitated a change to impeded flow [4, 11].

and Lock. The location of the chasm corresponds to a diametral Rayleigh number $Ra_d = 10^{5.5}$, a value almost identical to that found from chasmic data for the open thermosyphon [4]. The existence of this chasm remains to be explained, but the fact that it appears in both the open and closed system suggests that it is not associated with coupling. However, since it has also been observed in an open system with a central tube supplying a superimposed forced flow, the phenomenon appears to be associated with entry conditions near a mouth, real or false [6]. The change in heat transfer rate is dramatic, and it is tempting to suggest a choking stagnation mechanism in which interference between the boundary layer at its thickest point, and the core at its narrowest point, destabilize the flow into an unstructured motion until it is re-established in either the impeded or laminar boundary layer regime.

The current air data shown in Fig. 4 appear on the left-hand side of the chasm and support the prediction that they are in an impeded regime: the dashed line drawn through them has the slope of 1.0 characteristic of this regime. However, as the error bars indicate, the data are only qualitative and are not extensive enough to show the falling off expected as the chasm is approached. It is interesting to note that the current air and water data fall almost exclusively outside of the chasm.

Effect of geometry

The water data also appear to exhibit a chasmic transition, at least one side of it. This is noticeable in Fig. 4, and more clearly in Fig. 5. Such a rapid change in heat transfer rate has not been observed in water before, probably because Ra_d and t_d were too high. In view of the proximity to the critical value of t_d for air, it is tempting to suggest that the phenomenon has the same origin. It is clearly not the result of a normal transition from boundary layer to impeded flow, as the error bars indicate.

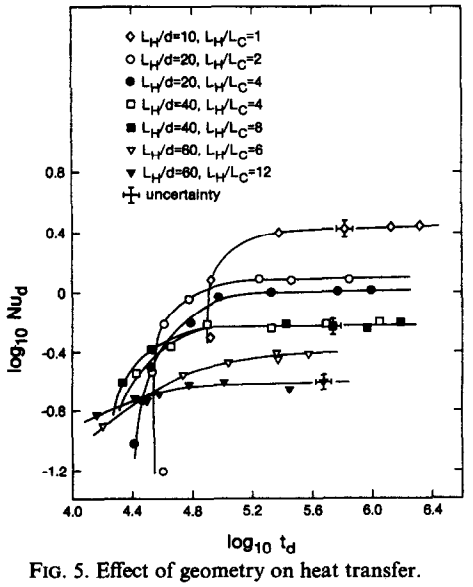

FIG. 5. Effect of geometry on heat transfer.

One possible explanation may be that $Ra_\Delta \ll Ra_\Delta^*$ and the flow is becoming increasingly refluent, but, if so, the air data should show similar behaviour. However, even though qualitative, the air data reveal Nusselt numbers comparable with those of boundary layer flow. An alternative explanation may be found in Fig. 3. The temperature records showed that the heated section wall never had temperatures less than 10°C, and therefore conditions corresponding to Fig. 3(c) never arose. However, the cooled section temperature did fall below 4°C for the lowest few points on each Nu_d–t_d curve. It therefore appears that these latter points correspond to the flow system depicted in Fig. 3(b), which is evidently a transitional regime between the advective cross coupling characteristic of high temperature differences (Fig. 3(a)) and the pure conduction of lower temperature differences when advection is completely absent. Among common fluids, such behaviour may be unique to water.

Figure 5 reveals that tube geometry has a significant effect on the location of this transitional regime. Given the above explanation, this dependency would be expected if the transition spanned only a narrow range of t_d, essentially determined by the Rayleigh number range in which $T_C < 4°C$. Thus, corresponding to the limited range of $T_H - T_C$ in which $T_C < 4°C$, there should be a limited range of t_d, the location of which on the t_d axis is inversely proportional to the length–diameter ratio, and essentially independent of the heated–cooled length ratio (which does not enter into the definition of Ra_d or t_d). Figure 5 is consistent with such behaviour and thereby offers support to the suggested model of the transition regime in near-freezing water. The more common transition to the impeded regime would be expected if $T_C > 4°C$.

Most of the points above the transition regime in Fig. 5 correspond to $T_C > 4°C$ and therefore the effect of inversion may generally be ignored in the interpretation of geometrical effects in the boundary layer regime. Consider first the effect of heated–cooled length ratio. Whenever this ratio departs from unity the longitudinal symmetry of the system is lost and the flow systems in the upper and lower sections will no longer be mirror images. For any given heat flux, the thickness of the annular stream (and core) in each section will generally be different across the junction plane, thus altering the details of the coupling process in accord with the tube geometry. Such changes must be compatible with corresponding changes in the flow system deep within each section.

When $L_H/L_C > 1$, the descending annulus in the cooled section will be thinner than the heated ascending annulus. Ideally, in the limiting case as $L_H/L_C \to \infty$, circulation in the heated section becomes completely refluent and the heat transfer rate of the entire system is controlled by conduction across the junction plane which then coincides with the top of the upper section. As L_H/L_C is decreased from the limiting value,

the rate of conduction increases as the cooled tube surface increases but it is not until an advective breakthrough occurs that the thermal exchange mechanism and the corresponding heat transfer efficiency change significantly. An increase in L_H/L_C may thus be viewed as a tendency towards increasingly refluent behaviour, thereby increasing the overall thermal impedance of the system. This reduction in performance is detectable in Fig. 5 from which it appears that the greater the increase in L_H/L_C (for a given value of L_H/d) the greater is the reduction in heat transfer. An apparent exception to this trend is seen in the data for $L_H/d = 40$, but the experimental error is too great to establish a contradiction to the expected trend, and $L_H/d = 40$ has a special significance, as noted later.

The effect of length–diameter ratio on heat transfer is much greater. Using the same flow model, it is to be expected that an increase in L_H/d would decrease the heat transfer rate, all other variables being held fixed, because of the effect produced in the coupling region. Since

$$\frac{\delta}{d} \simeq 1/t_d^{1/4}$$

in the laminar boundary layer regime, it is evident that increasing the tube length will create a thicker and slower boundary layer and hence the coupling mechanism will likely be less advective and more refluent. This is evidently a strong trend, as Fig. 5 shows.

Bayley and Lock [3] have used a Karman–Pohlhausen integral method to analyse the heat transfer performance of the closed tube thermosyphon under laminar, boundary layer conditions. For two particular coupling mechanisms, they were able to explore the effect of tube geometry. Their predictions and their experimental results indicate that the effect of length–diameter ratio and the effect of heated–cooled length ratio are both monotonic. The present experimental results confirm and extend these findings. This suggests that an empirical correlation in the form

$$Nu_d = a\left(\frac{L_H}{d}\right)^m \left(\frac{L_H}{L_C}\right)^n t_d^p \qquad (1)$$

may be made to fit the data of Fig. 5. Ignoring the transitional data, the effect of t_d is seen to be very small, i.e. $p \ll 1$. The value of 1/4, characteristic of laminar boundary layers, is not achieved, and this may be the result of temperature dependent properties (Pr in particular) between 0 and 80°C. Such dependency would certainly lower the local heat transfer coefficients with increasing temperatures, and may also permit greater secondary conduction.

Figure 6 shows the correlation when $L_H/d \leqslant 40$ and $L_H/L_C \leqslant 4$. The scatter is within the experimental error of $\pm 6\%$. This fit gives $m = -0.81$, $n = -0.26$ and $a = 11.75$, with $p = 0.03$. It is interesting to note that $m \simeq 3n$, as found in previous work with methanol [10]

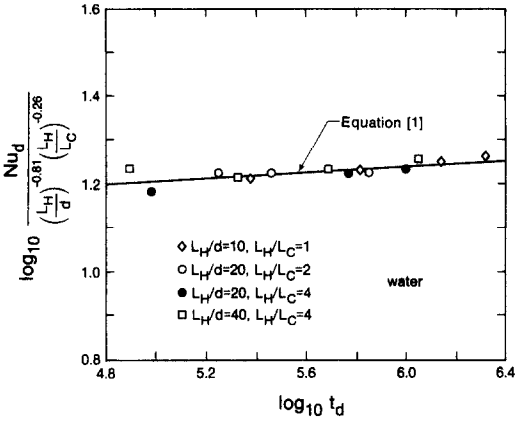

FIG. 6. Empirical heat transfer correlation: $L_H/d \leqslant 40$.

but under turbulent boundary layer conditions. This suggests that the geometrical group $(d/L_H)^3 L_C/L_H$ may have some significance. Figure 7 shows the correlation when $L_H/d \geqslant 40$ and $L_H/L_C \geqslant 6$. The standard deviation is about the same as in Fig. 6 but now $m = -1.65$, $n = -0.65$ and $a = 692$: p is again 0.03. It would appear that the data of Figs. 6 and 7 represent two different flow regimes distinguished not through t_d but through tube geometry: transition appears to occur near $(L_H/d)^3 L_H/L_C = 3 \times 10^5$. It is suggested that the exponents in Fig. 7 reflect the substantially increased influence of tube geometry in defining the coupling mechanism in the laminar boundary layer regime. Figure 8 satisfactorily compares the data of all seven runs with equation (1).

CONCLUSIONS

The effect of geometry on the heat transfer performance of the closed tube thermosyphon has been investigated at low Rayleigh numbers. This extends the previous work of Lock and Simpson [10] and Bayley and Lock [3] down into the laminar boundary layer regime, and beyond, thereby providing estimates

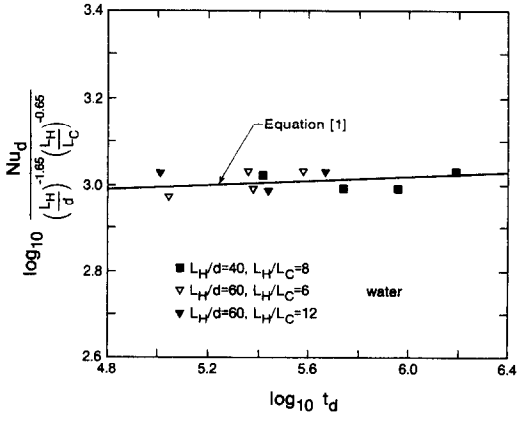

FIG. 7. Empirical heat transfer correlation: $L_H/d \geqslant 40$.

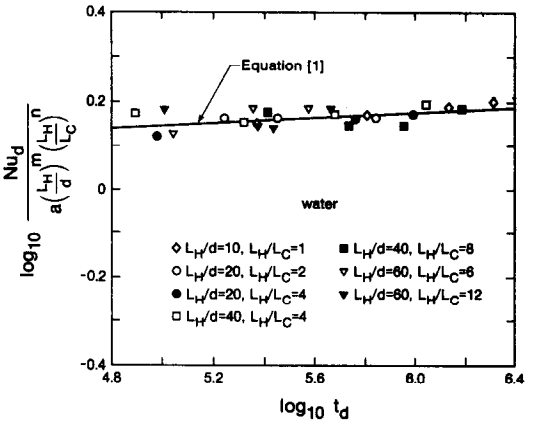

FIG. 8. Empirical heat transfer correlation: all data.

of system performance which are characteristic of small temperature differences. Apart from providing conservative heat transfer data useful for design purposes, the experiments also shed some light on the complex regime behaviour.

Although no attempt was made to systematically investigate the effect of Prandtl number, tests were undertaken with air and water fillings; the latter, the majority, included conditions under which the inversion temperature was spanned. The air data were only qualitative, and fell in the impeded regime. Nusselt numbers measured for air were comparable with those for water but were separated from the latter by a distinctive chasm, the origin of which is not precisely known. The water data fell mostly in the laminar boundary layer regime where they were noticeably below previous data. At their lower end, the water data did not exhibit the normal transition to impeded flow, but instead revealed a very sharp reduction in Nusselt number. This has been attributed to the change in internal flow pattern resulting from cooled water temperatures less than the inversion temperature.

The effect of tube geometry has been investigated in terms of the heated–cooled length ratio and the length–diameter ratio. The former ratio proved to have rather a weak monotonic effect: as L_H/L_C increased, Nu_d decreased, consistent with the flow model suggested. The length diameter ratio was found to have a much greater effect, exhibited in two ways. Firstly, the location of the transitional t_d range was lowered as L_H/d increased: this is consistent with the proposed effect on inversion. Secondly, the Nusselt number decreased as L_H/d increased, again in accord with the suggested coupling processes. These monotonic effects are in accord with previous studies of the closed tube thermosyphon, and have been represented in an empirical correlation of power law form suitable for application to laminar boundary layer conditions. This correlation indicates a further regime subdivision, evidently defined by tube geometry.

Acknowledgements—This work was undertaken with the aid of a grant from the Natural Sciences and Engineering Research Council of Canada to whom we are grateful. We also wish to thank Mr J. D. Kirchner for his assistance.

REFERENCES

1. G. F. Biyanov, V. I. Makarov and A. D. Molochnikov, Liquid cooling unit for freezing thawed ground and cooling plastically frozen ground for construction in areas with harsh climates, *Proc. 2nd Int. Permafrost Conf.*, N.A.S., p. 641 (1973).
2. G. S. H. Lock, The BIVA project, *Proc. IAHR Ice Symp.*, Vol. II, pp. 269–280 (1986).
3. F. J. Bayley and G. S. H. Lock, Heat transfer characteristics of the closed thermosyphon, *J. Heat Transfer* **87**, 30–40 (1965).
4. B. W. Martin, Free convection in an open thermosyphon tube with special reference to turbulent flow, *Proc. R. Soc.* **A230**, 502–530 (1955).
5. R. L. Reid, J. S. Tennant and K. W. Childs, The modelling of a thermosyphon type permafrost protection device, *J. Heat Transfer* 382–386 (1975).
6. G. S. H. Lock and J. D. Kirchner, Wind-augmented heat transfer in an open thermosyphon tube with large length–diameter ratios, *Proc. 27th Natl Heat Transfer Conf.*, ASME (1988).
7. G. S. H. Lock and J. D. Kirchner, Performance of an air-filled, open thermosyphon tube with particular reference to wind augmentation, *Int. J. Heat Mass Transfer* **31**, 2357–2364 (1988).
8. D. Japikse and E. R. F. Winter, Heat transfer and fluid flow in the closed thermosyphon, *Int. J. Heat Mass Transfer* **14**, 427–441 (1971).
9. G. A. S. Simpson, Geometrical effects in the closed tube thermosyphon, M.Sc. thesis, University of Alberta (1986).
10. G. S. H. Lock and G. A. S. Simpson, Performance of a closed tube thermosyphon with large length–diameter ratios, *Proc. 6th Int. OMAE Conf.*, Vol. IV, pp. 69–77 (1987).
11. M. J. Lighthill, Theoretical considerations on free convection in tubes, *Q. J. Mech. Appl. Math.* **6**(4), 398–439 (1953).
12. D. Japikse, Heat transfer in open and closed thermosyphons, Ph.D. thesis, Purdue University (1968).

EFFET DE LA GEOMETRIE SUR LES PERFORMANCES D'UN THERMOSIPHON TUBULAIRE FERME, AUX FAIBLES NOMBRES DE RAYLEIGH

Résumé—On présente les résultats d'une étude expérimentale du transfert thermique dans un thermosiphon tubulaire fermé pour des conditions laminaires. On porte attention sur l'effet de la géométrie du tube lorsque le nombre de Rayleigh est suffisamment faible pour créer des écoulements à couche limite, de transition ou génés. Les résultats montrent que le rapport longueur-diamètre et le rapport de la longueur chauffée sur la longueur refroidie ont tous les deux un effet monotone sur le transfert de chaleur, le premier étant le plus grand. Les données présentées concernent l'air et l'eau, avec des essais incluant l'effet de température de paroi refroidie suffisamment basse pour produire un renversement de l'écoulement dans la zone froide.

DER GEOMETRIEEINFLUSS AUF DIE LEISTUNG EINES GESCHLOSSENEN THERMOSYPHONS BEI KLEINER RAYLEIGH-ZAHL

Zusammenfassung—Es werden die Ergebnisse einer experimentellen Untersuchung des Wärmeübergangs in einem geschlossenen Thermosyphon unter laminaren Strömungsbedingungen vorgestellt. Dabei wird insbesondere der Einfluß der Rohrgeometrie berücksicht, wenn die Rayleigh-Zahl ausreichend klein für eine Grenzschichtströmung, einen Übergangsbereich und Strömungsbehinderungen ist. Die Ergebnisse zeigen, daß die Verhältnisse von Länge zu Durchmesser und von beheizter zu gekühlter Länge einen monotonen Einfluß auf den Wärmeübergang aufweisen. Als Arbeitsfluide wurden Luft und Wasser verwendet; bei Wasser ergab sich für sehr tiefe Wandtemperaturen eine Strömungsumkehr in der Kühlzone.

ВЛИЯНИЕ ГЕОМЕТРИИ НА РАБОЧИЙ РЕЖИМ ЗАМКНУТОГО ТРУБЧАТОГО ТЕРМОСИФОНА ПРИ НИЗКИХ ЧИСЛАХ РЭЛЕЯ

Аннотация—Представлены результаты экспериментального исследования теплопереноса в замкнутом трубчатом термосифоне при ламинарных условиях. Особое внимание обращается на влияние геометрии трубы для случая малых числе Рэлея, недостаточных для образования пограничного слоя, переходного режима и в условиях запирания течения. Данные показывают, что интенсивность теплопереноса монотонно растет с увеличением отношений длины к диаметру и длины нагреваемого участка к длине охлаждаемого. Представлены результаты для воздуха и воды, учитывающие роль температур охлаждаемых стенок, недостаточных для образования возвратного течения на участке отвода тепла.